Effects of Rapid Buffers on Ca^{2+} Diffusion and Ca^{2+} Oscillations

John Wagner and Joel Keizer
Institute of Theoretical Dynamics, Section of Neurobiology, Physiology, and Behavior, and Graduate Group in Applied Mathematics, University of California, Davis, California 95616, USA

ABSTRACT Based on realistic mechanisms of Ca^{2+} buffering that include both stationary and mobile buffers, we derive and investigate models of Ca^{2+} diffusion in the presence of rapid buffers. We obtain a single transport equation for Ca^{2+} that contains the effects caused by both stationary and mobile buffers. For stationary buffers alone, we obtain an expression for the effective diffusion constant of Ca^{2+} that depends on local Ca^{2+} concentrations. Mobile buffers, such as fura-2, BAPTA, or small endogenous proteins, give rise to a transport equation that is no longer strictly diffusive. Calculations are presented to show that these effects can modify greatly the manner and rate at which Ca^{2+} diffuses in cells, and we compare these results with recent measurements by Allbritton et al. (1992). As a prelude to work on Ca^{2+} waves, we use a simplified version of our model of the activation and inhibition of the IP_3 receptor Ca^{2+} channel in the ER membrane to illustrate the way in which Ca^{2+} buffering can affect both the amplitude and existence of Ca^{2+} oscillations.

INTRODUCTION

Calcium concentrations are strongly buffered in living cells. Buffer site concentrations have been estimated to be in the range of 100–300 μM in the cytoplasm and significantly higher in the endoplasmic reticulum (ER) (Allbritton et al., 1992; Milner et al., 1992). Although the majority of buffers are relatively stationary, Neher and colleagues (Zhou and Neher, 1993) have estimated that as much as 25% of cytoplasmic buffers in chromaffin cells are mobile with a molecular weight of the order of 15 kDa. The time constant for buffering has been estimated to be in the millisecond range or smaller, so that locally in space the concentration of free Ca^{2+}, $[Ca^{2+}]$, is determined by the association dissociation equilibrium with the buffers. The effect of this equilibrium is to distribute the Ca^{2+} between mobile and immobile pools, which has an enormous effect on the transport properties of Ca^{2+}: *the mobile buffers carry Ca^{2+} along, and the stationary buffers immobilize it.* Thus, commonly used exogenous buffers, like BAPTA, or mobile fluorescent indicators, like fura-2, can reduce the effect of endogenous buffers and, so speed up the transport of Ca^{2+}.

A number of previous experimental and theoretical studies have been carried out to assess the effect of buffering on Ca^{2+} concentrations in localized areas of cells. Of primary interest, especially in the early work, was estimating the concentration of cytosolic Ca^{2+} near the inner face of Ca^{2+} channels (Chad and Eckert, 1984; Fogelson and Zucker, 1985; Simon and Llinas, 1985). This has been significant in assessing the relevance of the shell (Eckert and Chad, 1984) and domain models (Sherman et al., 1990) of Ca^{2+}-induced inactivation of Ca^{2+} channels. This work has continued, with recent research focusing on the extent of Ca^{2+} domains (Llinas et al., 1992; Stern, 1992), their penetration into the interior of cells (Nowycky and Pinter, 1993), and the effect of exogenous Ca^{2+} buffers, such as BAPTA and fluorescent indicators, on Ca^{2+} dynamics (Blumenfeld et al., 1992; Hernandez-Cruz et al., 1990; Sala and Hernandez-Cruz, 1990; Roberts, 1993; Roberts, 1994). Because Ca^{2+} that enters a cell via ion channels redistributes itself throughout the cell via diffusion, the influence of buffers on the otherwise rapid diffusion of Ca^{2+} in aqueous media has been a key issue (Hodgkin and Keynes, 1957; Nowycky and Pinter, 1993; Allbritton et al., 1992).

The issue of how buffers affect the movement of Ca^{2+} in cells has recently arisen in the context of Ca^{2+} signaling from internal stores. Inositol 1,4,5-trisphosphate (IP_3), produced by agonist-mediated receptors in the plasma membrane, is a potent effector of Ca^{2+} release from the ER (Berridge, 1989). This mechanism is now widely believed to be a key feature of Ca^{2+} oscillations in a number of cell types, including hamster and *Xenopus* oocytes (Lechleiter and Clapham, 1992; Miyazaki et al., 1992; Nuccitelli et al., 1993), gonadotrophs (Li et al., 1994; Stojilkovic et al., 1993; Tse and Hille, 1991), RBL cells (Meyer and Stryer, 1991), and other cell types (Berridge, 1989). Mathematical modeling of the kinetics of the IP_3 receptor/Ca^{2+} channel (De Young and Keizer, 1992; Keizer and De Young, 1994; Li and Rinzel, 1994) in the ER has reinforced the notion that the coagonist properties of Ca^{2+} (Bezprozvanny et al., 1991; Finch et al., 1991) in conjunction with pumping by the ER's Ca^{2+} ATPase pump can explain the oscillations. In oocytes and other large cells, these oscillations often occur in conjunction with Ca^{2+} waves (Lechleiter and Clapham, 1992). To understand these phenomena, knowledge of the effect of endogenous Ca^{2+} buffers, as well as exogenous buffers and indicators, which are important tools in studying Ca^{2+} release, is essential. To understand the propagation speed, the frequency, and the amplitude of Ca^{2+} waves, the in situ magnitudes of the diffusion constant of both Ca^{2+} and IP_3 are also important

Received for publication 28 January 1994 and in final form 13 April 1994.
Address reprint requests to Joel E. Keizer, Institute of Theoretical Dynamics, University of California, Davis, CA 95616-8618. Tel.: 916-752-0938; Fax: 916-752-7297; E-mail: jekeizer @ucdavis.edu.

0006-3495/94/07/447/10 $2.00

(Allbritton et al., 1992; Lechleiter and Clapham, 1992; Mironov, 1990).

We report here a simplified description of these effects that is valid when the association dissociation equilibrium of the buffers is rapid with respect to diffusion. This condition is met by a number of important endogenous and exogenous buffers and allows for great simplification in the equations that describe the movement of Ca^{2+}. Instead of a reaction-diffusion-type equation with a constant diffusion coefficient coupled to other differential equations for the mobile and stationary buffers, we find that only a single nonlinear transport equation is required. This equation describes the time rate of change of the Ca^{2+} concentration and, in the case of stationary buffers alone, gives rise to a diffusion equation with a Ca^{2+}-dependent diffusion coefficient. In the presence of stationary and mobile buffers, the transport equation also contains terms that involve the diffusion coefficients of the mobile buffers and is more complex. Eliminating the shortest time scales allows larger time steps when numerically solving the reduced equations.

In addition to simplifying the dynamic description of buffering, this formalism allows us to define and calculate an effective diffusion constant for Ca^{2+} under a variety of conditions. We use these ideas to compare our calculations with in vitro diffusion measurements on *Xenopus* oocyte cytoplasm (Allbritton et al., 1992). We also derive expressions for the limiting values of the diffusion constant at low Ca^{2+} concentrations, examine the dependence of the diffusion constant on the percentage of mobile buffer, and determine the range of concentrations at which fura-2 might alter diffusion of Ca^{2+} within cells. Finally, in preparation for our treatment of Ca^{2+} buffering effects on Ca^{2+} waves, we carry out calculations using a model of IP_3-induced Ca^{2+} oscillations (De Young and Keizer, 1992; Li and Rinzel, 1994), with the nonlinear effects of buffering explicitly included. Changes in the amplitude, period, and existence of oscillations can be appreciable both for endogenous cytoplasmic and endogenous ER Ca^{2+} buffers.

EQUATIONS IN THE PRESENCE OF RAPID BUFFERING

In this section we consider the simplest case of Ca^{2+} buffering that includes both stationary and mobile buffers. We let B_i represent the buffer, where i = s or m represents stationary or mobile buffers, respectively. The buffer reactions are then

$$B_i + Ca^{2+} \underset{k_i^-}{\overset{k_i^+}{\rightleftharpoons}} CaB_i, \tag{1}$$

where CaB_i represents Ca^{2+} bound to a buffer site. Assuming mass action kinetics and Fickian diffusion (Keizer, 1987), we can immediately write the four transport equations that describe Ca^{2+} buffering:

$$\frac{\partial[Ca^{2+}]}{\partial t} = D_{Ca}\nabla^2[Ca^{2+}] - k_s^+[Ca^{2+}][B_s] + k_s^-[CaB_s] - k_m^+[Ca^{2+}][B_m] + k_m^-[CaB_m], \tag{2}$$

$$\frac{\partial[B_m]}{\partial t} = D_{B_m}\nabla^2[B_m] - k_m^+[Ca^{2+}][B_m] + k_m^-[CaB_m], \tag{3}$$

$$\frac{\partial[CaB_m]}{\partial t} = D_{CaB_m}\nabla^2[CaB_m] + k_m^+[Ca^{2+}][B_m] - k_m^-[CaB_m], \tag{4}$$

$$\frac{\partial[CaB_s]}{\partial t} = k_s^+[Ca^{2+}][B_s] - k_s^-[CaB_s], \tag{5}$$

where the $k_i^{\pm}$ are the association and dissociation rate constants; D_{Ca}, D_{B_m}, and D_{CaB_m} are the diffusion constants for free Ca^{2+}, mobile buffer, and Ca^{2+} bound to mobile buffer, respectively; and concentrations are represented by square brackets. These equations contain five time scales: the two time scales of the buffering and the three time scales of diffusion.

In what follows, we assume that the buffering time scales are rapid, reaching equilibrium at each point in space before appreciable diffusion occurs. This means that the buffering is a singular perturbation (Murray, 1989), which we handle by deriving an equation for the local, total concentration of Ca^{2+}, $[Ca^{2+}]_T$:

$$[Ca^{2+}]_T = [Ca^{2+}] + [CaB_s] + [CaB_m]. \tag{6}$$

By adding Eqs. 2, 4, and 5, we find that

$$\frac{\partial[Ca^{2+}]_T}{\partial t} = D_{Ca}\nabla^2[Ca^{2+}] + D_{CaB_m}\nabla^2[CaB_m]. \tag{7}$$

This equation does not involve the rapid buffering time scale and, therefore, involves no singular perturbation. It is possible to eliminate $[CaB_m]$ from this equation using the assumption of rapid equilibrium

$$[CaB_i] = \frac{[Ca^{2+}][B_i]_T}{K_i + [Ca^{2+}]}, \tag{8}$$

where K_i is the dissociation constant and $[B_i]_T$ is the total concentration of stationary or mobile buffer binding sites. When combined with Eq. 6, Eq. 8 allows $[Ca^{2+}]_T$ to be written in terms of $[Ca^{2+}]$:

$$[Ca^{2+}]_T = [Ca^{2+}]\left(1 + \frac{[B_s]_T}{(K_s + [Ca^{2+}])} + \frac{[B_m]_T}{(K_m + [Ca^{2+}])}\right). \tag{9}$$

As we show in Appendix A, Eqs. 7–9 can be used to obtain the following, single transport equation for free Ca^{2+}:

$$\frac{\partial[Ca^{2+}]}{\partial t} = \beta(D_{Ca} + \gamma D_{CaB_m})\nabla^2[Ca^{2+}] - \frac{2\beta\gamma D_{CaB_m}}{K_m + [Ca^{2+}]}\nabla[Ca^{2+}]\cdot\nabla[Ca^{2+}], \tag{10}$$

where

$$\beta = \left(1 + \frac{K_s[B_s]_T}{(K_s + [Ca^{2+}])^2} + \frac{K_m[B_m]_T}{(K_m + [Ca^{2+}])^2}\right)^{-1} \quad (11)$$

and

$$\gamma = \frac{K_m[B_m]_T}{(K_m + [Ca^{2+}])^2}. \quad (12)$$

Two additional conditions on the mobile buffers, derived in the Appendix, are required for this simplification: 1) the initial total concentration of the mobile buffer,

$$[B_m]_T = [B_m] + [CaB_m], \quad (13)$$

must be spatially uniform, and 2) the diffusion constants D_{CaB_m} and D_{B_m} must be approximately equal. These conditions seem to be reasonable for endogenous buffers with molecular masses above 1–2 kDa, and should be realistic for many exogenous mobile buffers, especially dextran associated fluorophores; they will be assumed true throughout the remainder of this work.

Note that in addition to the diffusive-appearing contribution of the first term in Eq. 10, there is a second term involving the square of the Ca^{2+} gradient. That term is less than or equal to zero for all gradients and, therefore, is nondiffusive. Indeed, it counteracts the diffusive-like movement of unbound Ca^{2+} given by the first term. In the absence of mobile buffer, $\gamma = 0$ and β simplifies to

$$\beta = \left(1 + \frac{K_s[B_s]_T}{(K_s + [Ca^{2+}])^2}\right)^{-1}. \quad (14)$$

In this case, the equation involves only a diffusion-like Laplacian term, albeit with a Ca^{2+}-dependent diffusion coefficient, *i.e.*,

$$\frac{\partial[Ca^{2+}]}{\partial t} = \left(1 + \frac{K_s[B_s]_T}{(K_s + [Ca^{2+}])^2}\right)^{-1} D_{Ca}\nabla^2[Ca^{2+}]. \quad (15)$$

A more complete understanding of the nondiffusive term in Eq. 10 can be obtained by writing that equation in the form of an equivalent conservation equation (Keizer, 1987). Defining the calcium-dependent diffusion constant as

$$D([Ca^{2+}]) = \beta\left(D_{Ca} + D_m \frac{K_m[B_m]_T}{(K_m + [Ca^{2+}])^2}\right) \quad (16)$$

and the diffusion flux as

$$j([Ca^{2+}]) = -D([Ca^{2+}])\nabla[Ca^{2+}], \quad (17)$$

it is possible to rearrange Eq. 10 into the form

$$\frac{\partial[Ca^{2+}]}{\partial t} = -\nabla \cdot j([Ca^{2+}]) - \frac{d\beta}{\beta d[Ca^{2+}]} D([Ca^{2+}])\nabla[Ca^{2+}] \cdot \nabla[Ca^{2+}]. \quad (18)$$

This is the standard form of a conservation equation in which the first term represents changes in the concentration of unbound Ca^{2+} ions caused by surface fluxes. Using Eq. 11, it is easy to show that the derivative $d\beta/d[Ca^{2+}]$ is non-negative. Thus, the second term in Eq. 18, which is the nondiffusive term, is never positive and, therefore, represents a *sink* for unbound Ca^{2+} ions. This nondiffusive sink term is a result of the uptake of Ca^{2+} by buffers that occurs when unbound Ca^{2+} ions move down their concentration gradient. Indeed, as long as $d\beta/d[Ca^{2+}] > 0$, a larger fraction of the ions that move down the gradient into the lower concentration region will be taken up by the buffers there than will be released from the buffers at the high concentration end of the gradient. Only when $d\beta/d[Ca^{2+}] \approx 0$, which occurs as a limiting case when $[Ca^{2+}]/K_i \ll 1$, does the nondiffusive sink term vanish. By using the explicit form for $j([Ca^{2+}])$ in Eq. 17, it is possible to decompose the first term in Eq. 18 to obtain

$$\frac{\partial[Ca^{2+}]}{\partial t} = -D([Ca^{2+}])\nabla^2[Ca^{2+}] - \left(\frac{dD}{d[Ca^{2+}]} + \frac{d\beta}{\beta d[Ca^{2+}]} D([Ca^{2+}])\right) \times \nabla[Ca^{2+}] \cdot \nabla[Ca^{2+}]. \quad (19)$$

This form of the equation makes it clear that the nondiffusive term in Eq. 10 has two components: one that arises from the dependence of the diffusion constant, $D([Ca^{2+}])$, on $[Ca^{2+}]$ and the other that arises from the sink effect described in Eq.18.

The validity of the rapid equilibrium approximation derived in the Appendix requires that the time scales for buffering be rapid with respect to the time scale of diffusion. The buffering time scales can be estimated by linearizing the terms for the association reaction around their equilibrium values, which gives

$$\tau_i = \frac{1}{k_i^- + k_i^+([Ca^{2+}] + [B_i])}. \quad (20)$$

The characteristic times for diffusion, on the other hand, depend on the gradients in the system and can be written

$$\tau_{dif} \approx L^2/D, \quad (21)$$

where L is a length characteristic of the spatial profile of the species with diffusion constant, D. Thus, the condition for the validity of the rapid equilibrium approximation can be written

$$\tau_i \ll L^2/D. \quad (22)$$

In the cytoplasm the diffusion constant of unbound Ca^{2+}, D_{Ca}, has been estimated (Allbritton et al., 1992; Zhou and Neher, 1993) to be about 225–300 $\mu m^2\ s^{-1}$. The diffusion constants for mobile cytoplasmic buffers can be estimated from their molecular masses, which appear (Zhou and Neher, 1993) to be in the range 7–20 kDa, to be a factor 2–10 smaller than that for Ca^{2+}. Diffusion constants for small exogenous buffers, such as BAPTA or fura-2, are probably smaller than that of Ca^{2+} (Timmerman and Ashley, 1986). If we assume

that a spatial profile of Ca^{2+} has a length scale of 5 μm, as might be typical of a sharp Ca^{2+} wave front, then Eq. 22 and these estimates of diffusion constants imply that the rapid equilibrium approximation should hold if equilibration times for the buffers are less than approximately 10 ms. In chromaffin cells, a time constant for stationary and mobile buffers of the order of 1 ms has been estimated using patch pipettes (Neher and Augustine, 1992), whereas from the values of $k_m^- = 97$ s and $k_m^+ = 601$ μMs^{-1} for fura-2, one estimates a relaxation time of the order of 5 ms. Thus, the rapid equilibrium approximation, as given by Eq. 8, should be a reasonable approximation for most in vivo measurements.

The approximation also can be tested numerically by integrating Eqs. 2–5 and comparing the result to Eq. 10. A typical result for purely stationary buffers is shown in Fig. 1, where an initial Gaussian pulse of Ca^{2+} ($[Ca^{2+}] = 1.78$ μM at maximum, width = 5 μm) was added to a uniform background of Ca^{2+} ($[Ca^{2+}]_0 = 0.1$ μM). The differences in $[Ca^{2+}]$ at times the order of a few milliseconds represents the breakdown of the approximation on small length and time scales. Note that as time proceeds, the approximation improves on all length scales. Calculations with the same dissociation constant, K_s, as in Fig. 1, but with larger values of the rate constants, exhibit an even shorter initial interval in which the two calculations are different.

The equations derived in this section are easily generalized when multiple types of stationary and mobile buffer sites are present, all participating in buffering by the association-dissociation reaction in Eq. 1. The resulting equations are given in Appendix B. In case some of the buffers are not rapid, then the ordinary differential equations that correspond to their slow kinetics (cf Eq. 1) must be solved along with the transport equation for $[Ca^{2+}]$.

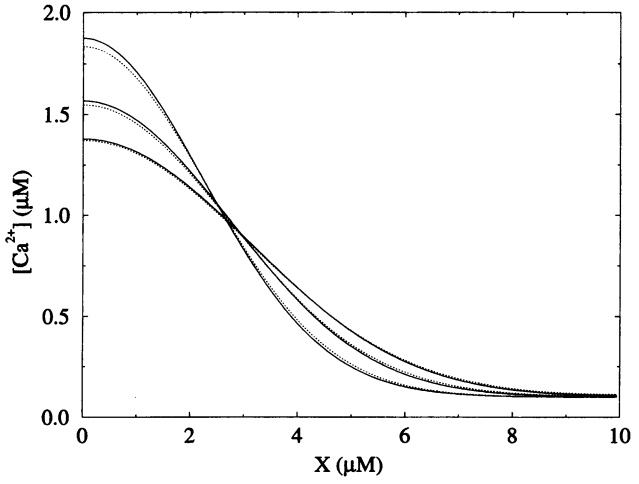

FIGURE 1 Plot of $[Ca^{2+}]$ distributions at $t = 1$ ms, $t = 50$ ms, and $t = 100$ ms for Eqs. 2–5 (*dashed curves*) and Eq. 10 (*solid curves*). Simulations assumed no mobile buffer, used a simple explicit integration scheme (forward difference in time, centered difference in space, with β evaluated at the center node), and parameter values $k_s^+ = 10$ $\mu M^{-1} s^{-1}$, $k_s^- = 100$ s^{-1}, $K_s = k_s^-/k_s^+ = 10$ μM, $D_{Ca} = 225$ $\mu m^2 s^{-1}$, $[B_s]_T = 114$ μM.

EFFECTIVE DIFFUSION CONSTANTS

Despite the complexity of Eq. 10, it is possible to derive expressions for effective diffusion constants for Ca^{2+} under a variety of different conditions. Because of the explicit appearance of $[Ca^{2+}]$ in Eq. 10, these expressions generally depend on $[Ca^{2+}]$. Consider first the simplest situation with only stationary buffers. In that case, Eq. 15 applies along with the simplified expression for β in Eq. 14. If we consider a small pulse of Ca^{2+}, released via a pipette or from caged Ca^{2+}, diffusing into a cytoplasmic background of concentration c_0, then these equations suggest that the effective diffusion constant of Ca^{2+} can be approximated by

$$D_{app} \approx \beta_0 D_{Ca} = \left(1 + \frac{K_s[B_s]_T}{(K_s + c_0)^2}\right)^{-1} D_{Ca}. \quad (23)$$

If c_0 is large compared to the pulse size, $[Ca^{2+}] \approx c_0$, and this approximation improves. In the limit of small c_0 or large K_s, this expression for D_{app} reduces to

$$D_{app} \approx \frac{K_s}{K_s + [B_s]_T} D_{Ca}, \quad (24)$$

which is useful for approximate calculations.

A numerical definition of D_{eff} can be derived from the diffusion equation. If the diffusion constant is actually a constant, the diffusion equation has a Gaussian solution for an initial Gaussian pulse into a background concentration, c_0. Indeed, for the initial condition

$$c(x, 0) = c_0 + (2\pi\sigma)^{-1/2}\exp(-x^2/(2\sigma)), \quad (25)$$

the solution of Fick's law (with D as a constant) is

$$c(x, t) = c_0 + (4\pi Dt + 2\pi\sigma)^{-1/2}\exp\left(-\frac{x^2}{4Dt + 2\sigma}\right), \quad (26)$$

where here, and in the remainder of the paper, we simplify notation by writing $[Ca^{2+}] = c$. After the spread of an initial Gaussian pulse, centered at the origin, we use Eq. 26 to define an effective diffusion constant for Eq. 10 as

$$D_{eff} \equiv \left\langle \frac{1}{4\pi t\,[c(0, t) - c_0]^2} - \frac{\sigma}{2t} \right\rangle, \quad (27)$$

where $\langle\cdot\rangle$ denotes a running time average over a short time interval centered at t.

We first apply this definition in the presence of stationary buffer alone using Eq. 15. That equation simplifies greatly if we change to the dimensionless variables: $c^* = (K_s + c)/\sqrt{K_s[B_s]_T}$, $x^* = x/L$, and $t^* = tD_{Ca}L^{-2}$, where $0 \le x \le L$. For one spatial dimension it takes the form

$$\frac{\partial c^*}{\partial t^*} = \frac{c^{*2}}{c^{*2} + 1}\frac{\partial^2 c^*}{\partial x^{*2}}. \quad (28)$$

Fig. 2 illustrates graphs of D_{eff}, calculated using Eq. 27, and the approximate expression given in Eq. 23 as functions of the background concentration, $c_0^* = (K_s + c_0)/\sqrt{K_s[B_s]_T}$. In terms of the dimensionless variable, c_0^*, the

approximate expression in Eq. 23 becomes

$$D_{app} \approx \frac{c_0^{*2}}{c_0^{*2} + 1} D_{Ca}, \quad (29)$$

which is shown as the full line in Fig. 2. Calculations with Eq. 28 were carried out with an implicit integration scheme (see Fig. 2) using values of $[B_s]_T = 100$ μM and $K_s = 1$ μM. Eq. 28, however, predicts that the calculations should give results independent of these values, a fact that we have verified numerically.

Notice in Fig. 2 that as c_0^* increases, the background Ca^{2+} saturates the buffer, thus decreasing the ability of the buffer to hinder the diffusion of Ca^{2+}. As expected, at high c_0^*, the approximate expression for D_{app} in Eq. 29 improves dramatically. From the nondimensionalization, we see that increasing K_s increases c_0^*, thereby increasing D_{eff}; increasing $[B_s]_T$, however, decreases c_0^*, thereby decreasing D_{eff}. The inset in Fig. 2 is a blow up of the region of physiological values of c_0^*. Although the relative error made in using D_{app} as an approximation to D_{eff} is as high as 50% in this region, the difference $D_{eff} - D_{app}$ remains fairly constant.

In the presence of mobile buffer, the reduced equation can be nondimensionalized by the same transformation if we assume that $K_s = K_m$. This yields

$$\frac{\partial c^*}{\partial t^*} = \frac{c^{*2} + B_r D_r}{c^{*2} + 1 + B_r} \frac{\partial^2 c^*}{\partial x^{*2}} - \frac{2B_r D_r}{c^*(c^{*2} + 1 + B_r)} \left(\frac{\partial c^*}{\partial x^*}\right)^2, \quad (30)$$

where $B_r = [B_m]_T/[B_s]_T$ and $D_r = D_{CaB_m}/D_{Ca}$. Thus, in the presence of mobile buffer, solutions of the diffusion equation will depend only on B_r and D_r, and we can characterize D_{eff} simply by specifying B_r and D_r. This is done in Fig. 3, where D_{eff}/D_{Ca} is given as a function of B_r for several values of D_r with $K_s = K_m = 5$ μM. Increasing the mobility of the buffer increases D_{eff} as does increasing the percentage of mobile buffer. This confirms our intuition that the mobile buffers assist Ca^{2+} transport by competing with the stationary buffers for Ca^{2+} binding and then carrying the bound Ca^{2+} along as they diffuse. The effect here can be significant, even when the total amount of mobile buffer is only of the order of 10% of the stationary buffer. As the three curves show, mobile buffers with much smaller diffusion constants than Ca^{2+} can increase the effective diffusion constant by factors of two to three. Based on experiments in chromaffin cells (Zhou and Neher, 1993), this suggests that mobile endogenous buffers will be an important factor in determining the rate at which Ca^{2+} moves.

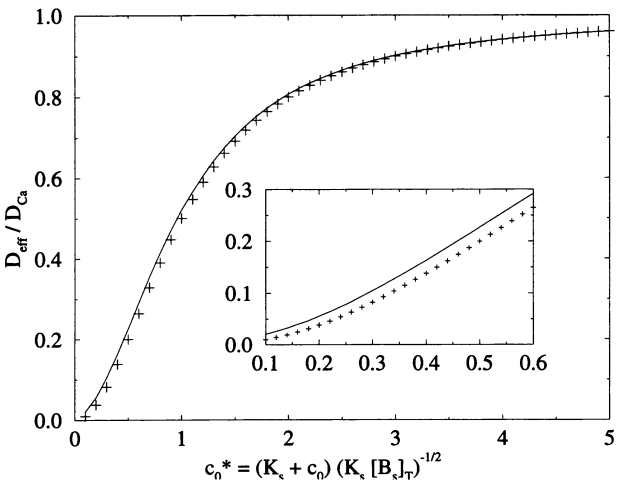

FIGURE 2 Plot of D_{eff}/D_{Ca} (*solid curve*) and D_{app}/D_{Ca} (+ + +) versus the dimensionless background Ca^{2+} concentration c_0^*. Inset shows physiological values of c_0^*. In these simulations, $[B_s]_T = 100$ μM, $K_s = 1$ μM, $D_{Ca} = 250$ $\mu m^2\ s^{-1}$ and no mobile buffer. Numerical integration scheme for this and remaining simulations used (implicit) Crank-Nicholson with β evaluated at the center node of the backward time.

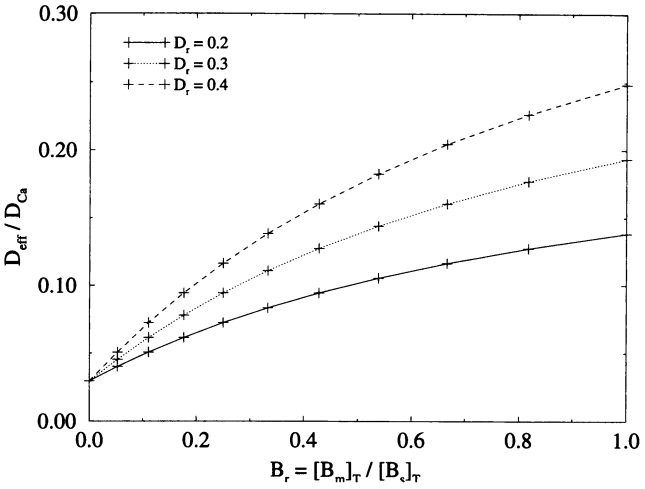

FIGURE 3 Plot of D_{eff}/D_{Ca} versus B_r for three values of D_r. Parameter values: $K_s = K_m = 5$ μM, $D_{Ca} = 250$ $\mu m^2\ s^{-1}$, $c_0 = 0.1$ μM, with $[B_s]_T$ and $[B_m]_T$ varied such that total buffer $[B_s]_T + [B_m]_T = 200$ μM.

APPLICATIONS OF THE THEORY

To demonstrate the utility of this formalism, we have applied it to several problems of current interest: the effect of mobile fluorescent indicators on Ca^{2+} diffusion; measurement of Ca^{2+} diffusion constants in the presence of endogenous buffers; and the effect of Ca^{2+} buffering on Ca^{2+} oscillations.

Mobile fluorescent indicators

We have investigated the effect of mobile indicators on Ca^{2+} diffusion using Eqs. 10 and 27 to calculate effective diffusion constants. We have used binding constants for the stationary buffers that are typical of those estimated in the cytoplasm and used the measured value of the dissociation constant for fura-2, $K_m = 0.16$ μM. Fura-2 is a mobile buffer and, therefore, its diffusion can affect the diffusive transport of Ca^{2+}. We have used a value of 50 $\mu m^2\ s^{-1}$ for the diffusion constant of fura-2, which is of the order of the value measured in smooth muscle cells (Timmerman and Ashley, 1986). Fura-2 is an appropriate choice for applying our formalism, not only because it is used extensively in experiment, but also because its rapid binding kinetics satisfy the time scale separation required by our formalism (Kao and Tsien, 1988). Given the

relative sizes of fura-2 and Ca^{2+}, it also appears likely that the diffusion constants of fura-2 with bound Ca^{2+} and free fura-2 are quite similar, which is the other assumption underlying Eq. 10.

Fig. 4 shows the results of the fura-2 simulations. In these simulations, we used $K_s = 10\ \mu M$, $K_m = 0.16\ \mu M$, $[B_s]_T = 150\ \mu M$, $D_{Ca} = 250\ \mu m^2\ s^{-1}$, $D_{CaB_m} = 50\ \mu m^2\ s^{-1}$, $c_0 = 0.1\ \mu M$, and varied $[B_m]_T$, the total concentration of fura-2, in the range 0–1 μM. The main graph illustrates the increase in the effective diffusion constant of Ca^{2+} as a function of the total concentration of fura-2. Even with the concentration of fura-2 as low as 1 μM, the effective diffusion constant is increased by about 30%. In this range, the increase with fura-2 concentration is approximately linear, which can be deduced from Eq. 10 using the approximate expression

$$D_{app} \approx \beta_0 \left(D_{Ca} + D_m \frac{K_m [B_m]_T}{(K_m + c_0)^2} \right), \tag{31}$$

where β_0 is evaluated at the background Ca^{2+} concentration, c_0. However, already at 10 μM, a concentration of fura-2 well below that often used experimentally, the diffusion constant is increased by more than a factor of 3, from 17 to 60 $\mu m^2\ s^{-1}$.

The insets illustrate another important feature of the simulations. The upper inset shows the time course of D_{eff}, calculated in the presence of 0.1 μM fura-2, far below values used experimentally. Note that D_{eff} achieves a constant value within about 20 ms, showing that the transport of Ca^{2+} rapidly becomes diffusive at this concentration. At higher concentrations, however, D_{eff} *does not achieve a constant value*, as shown at 10 μM fura-2 in the lower inset. These and similar calculations with larger values of D_{CaB_m} make it clear that the nondiffusive terms in Eq. 10 can be significant at concentrations of mobile buffer much smaller than the stationary buffer.

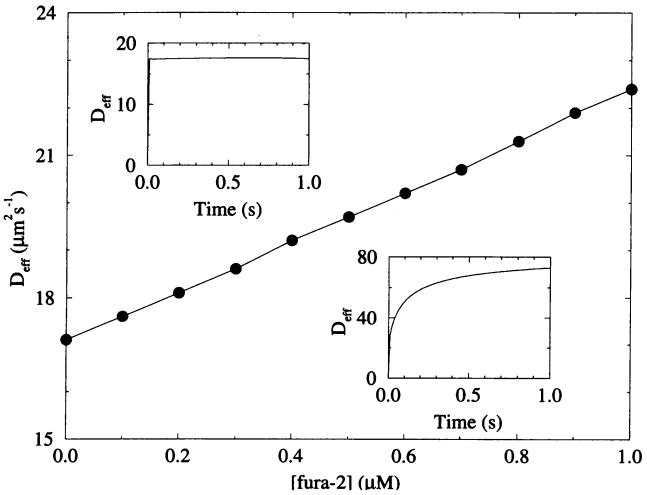

FIGURE 4 Plot of D_{eff} as a function of total fura-2 concentration, $[B_m]_T$. Insets show time series of D_{eff} for $[B_m]_T = 0.1\ \mu M$ (*upper inset*) and $[B_m]_T = 10\ \mu M$ (*lower inset*). Parameter values: $K_s = 10\ \mu M$, $K_m = 0.16\ \mu M$, $[B_s]_T = 150\ \mu M$, $D_{Ca} = 250\ \mu m^2\ s^{-1}$, $D_{CaB_m} = 50\ \mu m^2\ s^{-1}$, $c_0 = 0.1\ \mu M$.

It is possible to use Eq. 10 to estimate the conditions under which the nondiffusive second term in that equation becomes significant. We introduce the nondimensional variables $c^* = c/K_m$, $x^* = x/L$, and $t^* = tD_{Ca}L^{-2}$ into Eq. 10, where for fura-2 c^* is order of unity at physiological values of $[Ca^{2+}]$. This gives

$$\frac{\partial c^*}{\partial t^*} = \beta(1 + \gamma(D_{CaB_m}/D_{Ca}))\{\nabla^2 c^* - \alpha \nabla c^* \cdot \nabla c^*\}, \tag{32}$$

where

$$\gamma = \frac{[B_m]_T/K_m}{(1 + c^*)^2} \tag{33}$$

$$\alpha = \frac{2\gamma(D_{CaB_m}/D_{Ca})}{(1 + c^*)(1 + \gamma(D_{CaB_m}/D_{Ca}))}. \tag{34}$$

It is obvious from the form of Eq. 32 that it will behave like a diffusion equation with an approximate diffusion constant as long as the second term in the curley brackets is negligible compared with the first term. This will occur when

$$\alpha = \frac{2\gamma(D_{CaB_m}/D_{Ca})}{(1 + c^*)(1 + \gamma(D_{CaB_m}/D_{Ca}))} \ll 1. \tag{35}$$

Using Eqs. 33 and 34 and the fact that $c^* \approx 1$, we find that

$$\alpha \approx \frac{[B_m]_T/4K_m}{[B_m]_T/4K_m + D_{Ca}/D_{CaB_m}}. \tag{36}$$

The data for fura-2 given in the legend to Fig. 4 are easily used in this expression to determine the concentration of fura-2 at which the criterion in Eq. 35 breaks down. We find that this occurs when $[\text{fura-2}]_T \approx 0.6\ \mu M$, in good agreement with our simulations.

Although Eq. 35 only applies in the presence of a single type of mobile buffer, it is possible using Eq. 44 in the Appendix to show that the presence of low affinity endogenous mobile buffers ($K_m \geq 5\ \mu M$) does not change the criterion in Eq. 35 appreciably. We have also checked that the low affinity mobile buffers used in the calculations given in Fig.3 do not cause the effective diffusion constant calculations to break down except when their concentration is large. We find, in general, that the lower the affinity of the mobile buffers, the better the effective diffusion approximation becomes.

In vitro measurements

We have carried out calculations that simulate the in vitro measurements by Allbritton *et al.* (1992) of the diffusion constant of Ca^{2+} in cell-free extracts from *Xenopus laevis* oocytes. After calcium handling by the ER and mitochondria was inhibited, diffusion of Ca^{2+}, presumably only in the presence of endogenous buffers, was monitored using $^{45}Ca^{2+}$ as a tracer. By layering the tracer at one end of a tube and following its progress over time, profiles of Ca^{2+} concentration, normalized to the maximum value at the origin, were obtained.

We have simulated this experiment directly using Eq. 10 with an initial 44-μM pulse of Ca^{2+} at the origin and a background Ca^{2+} concentration of $c_0 = 0.1$ μM, similar to the values used in the experiment (Allbritton et al., 1992). We have used a range of plausible values for D_{Ca}, D_m, dissociation constants, and buffer concentrations in these calculations. A typical result is shown in Fig. 5. That calculation included predominately stationary buffers ($K_s = 8.3$ μM, $[B_s]_T = 114$ μM), and only a small amount of exogenous mobile buffer ($K_m = 0.16$ μM, $[B_m]_T = 0.1$ μM, and $D_{CaB_m} = 250$ $\mu m^2 s^{-1}$), and $D_{Ca} = 250$ $\mu m^2 s^{-1}$. The amount of mobile buffer, which has a smaller effect on these calculations than the stationary buffer, was purposely kept small in this example to avoid the nondiffusive contributions of the sort illustrated in Fig. 4. In Fig. 5, the solid curves represent the normalized Ca^{2+} profile calculated at 15-min intervals using Eq. 10. These results are in reasonable agreement with experimental results on cell free extracts (Allbritton et al., 1992). For comparison, Eq. 31 was used to define an apparent diffusion coefficient, $D_{app} = 21.1$ $\mu m\ s^{-1}$, for this simulation. The dashed curves in Fig. 5 illustrate the resulting Gaussian curves that come from solving the diffusion equation with this constant value for the diffusion constant. Although this approximation gives a slightly faster rate of spread for the Ca^{2+} profile, it does a reasonable job of approximating the complete calculations. Thus, under appropriate conditions of mobile buffer, Eq. 31 should be a reasonable approximation (Zhou and Neher, 1993).

We have been able to calculate values of the effective diffusion constant for Ca^{2+} that are comparable with those reported experimentally in this preparation using the following diffusion and buffer constants: $D_{Ca} = 370$ $\mu m^2 s^{-1}$, $[B_s]_T = 85.5$ μM, $K_s = 6$ μM, $[B_m]_T = 28.5$ μM, $K_m = 6$ μM, and $c_0 = 0.1$ μM. For these values we find that $D_{eff} = 38$ $\mu m^2 s^{-1}$. The mobile buffer in this case is assumed to be endogenous, with $[B_m]_T$ taken to be 25% of the total endogenous buffer and $D_{CaB_m} = 75$ $\mu m^2 s^{-1}$. Decreasing K_s and K_m to 1 μM lowered the value of D_{eff} to 27 $\mu m^2 s^{-1}$, whereas increasing K_s and K_m to 10 μM yielded $D_{eff} = 49$ $\mu m^2/s$; these latter values represent the low and high ends of the statistical tolerance levels for the measured values of D_{Ca} reported in (Allbritton et al., 1992). These low and high values of K_s correspond to the experimental estimates of the extreme values for the buffering dissociation constant, calculated by measuring free Ca^{2+} after adding different amounts of Ca^{2+} to extracts (Allbritton et al., 1992).

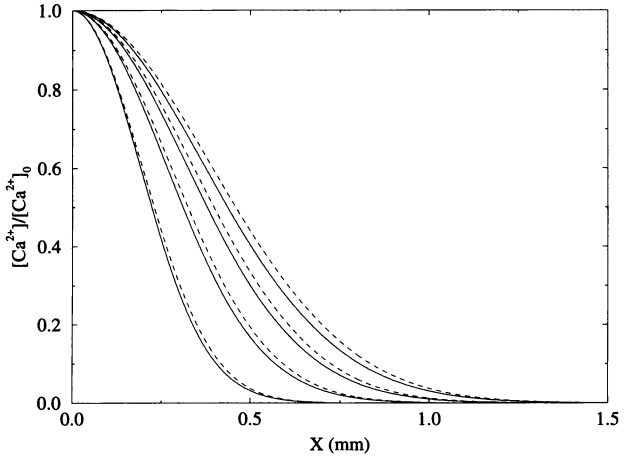

FIGURE 5 Solid curves are plots of normalized $[Ca^{2+}]$ distributions at 15-min intervals for an initial 44 μM Ca^{2+} pulse at the origin. Dashed curves are Gaussians that result from a constant diffusion constant, $D_{app} = 21.1$ $\mu m^2 s^{-1}$. Parameter values: $K_s = 8.3$ μM, $K_m = 0.16$ μM, $[B_s]_T = 114$ μM, $[B_m]_T = 0.1$ μM, $D_{Ca} = 250$ $\mu m^2 s^{-1}$, $D_{CaB_m} = 250$ $\mu m^2 s^{-1}$, $c_0 = 0.1$ μM.

Buffering effects on Ca^{2+} oscillations

Exogenous buffers have been shown to alter the speed of Ca^{2+} waves in mature *Xenopus* oocytes (Nuccitelli et al., 1993), an effect that might be related to the various buffering terms in Eq. 10. One effect of buffering persists even if the concentration of Ca^{2+} is spatially uniform. In this case Eq. 38 becomes

$$\frac{d[Ca^{2+}]_T}{dt} = \frac{1}{\beta}\frac{d[Ca^{2+}]}{dt} = J, \tag{37}$$

where J represents the rates of other mechanisms that transport Ca^{2+} into or out of the cytoplasm. Here, as a preliminary to treating Ca^{2+} waves, we explore the effect of buffering on a recent mechanism that has been used to explain IP_3-induced Ca^{2+} oscillations (De Young and Keizer, 1992).

We employ a simplified two variable version of the De Young-Keizer model (Li and Rinzel, 1994) that accurately reproduces the original model. Details of the model, including the influence of buffering of Ca^{2+} in the cytoplasm and ER, are given in Appendix C. The effects of buffering in this model are most easily seen by examining bifurcation diagrams. Two such diagrams are given in the main graphs in Fig. 6, which show the steady state values of $[Ca^{2+}]$ calculated from the kinetic equations, Eqs. 47–49 as a function of the parameter $[IP_3]$. Two types of steady states are represented: stable steady states, represented by a single line, and stable oscillations, represented by the maximum and minimum values of $[Ca^{2+}]$ in the oscillation. The insets show similar bifurcation diagrams for the buffering function, $\beta(c)$. The "bubble" structure in the diagrams begins and ends at points of Hopf bifurcations, where the steady states lose or regain their stability.

Using $[IP_3]$ as the bifurcation parameter, we found that the range of $[IP_3]$ values for which the model exhibited calcium oscillations depends strongly on the buffering dissociation constants in the cytosol, K_{cyt}, and the ER, K_{ER}. For example, for $K_{cyt} = 0.75$ μM and $[B_{cyt}] = 150$ μM, oscillations occurred in the range $0.419\ \mu M \le [IP_3] \le 0.646\ \mu M$, whereas increasing K_{cyt} to 1.50 μM produced oscillations for $0.347\ \mu M \le [IP_3] \le 0.837\ \mu M$. Furthermore, increasing K_{cyt} increased the amplitude of the oscillations, the maxima increasing and the minima decreasing, across the entire range of $[IP_3]$.

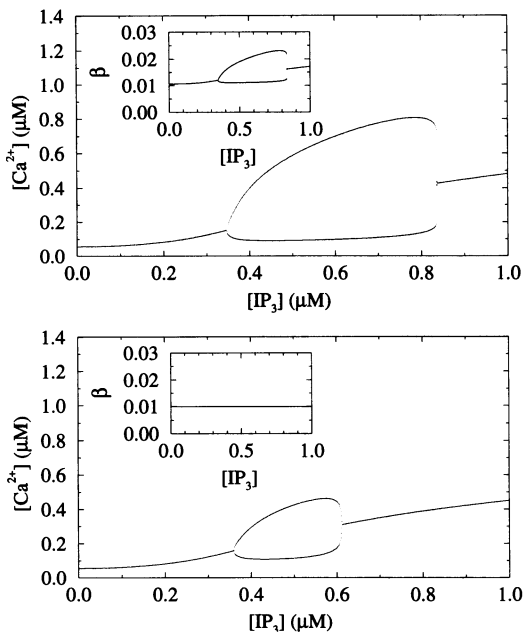

FIGURE 6 Plot of steady-state values of $[Ca^{2+}]$ as a function of the bifurcation parameter $[IP_3]$, as explained in text. *Upper panel* buffering parameters K_{cyt} = 1.5 μM, $[B_{cyt}]$ = 150 μM. (*Lower panel*) K_{cyt} = 150 μM, $[B_{cyt}]$ = $1.5 \cdot 10^4$ μM. All other parameters as in Appendix C. Insets are bifurcation plots for $\beta(c)$.

Increasing K_{cyt} with $[B_{cyt}]$ fixed increases the average fraction of free calcium. Fig. 6 illustrates the effects of increasing K_{cyt} and $[B_{cyt}]$ with $K_{cyt}/[B_{cyt}]$ fixed at 0.01. In the top plate of Fig. 6, K_{cyt} = 1.5 μM and $[B_{cyt}]$ = 150 μM. For these values, which are realistic biophysically, oscillations begin at $[IP_3]$ = 0.347 μM and terminate at $[IP_3]$ = 0.837 μM and are of large amplitude. The inset to that figure shows that the buffering factor, $\beta(c)$, also oscillates, changing its value by a factor of two or more. Indeed, to insure that oscillations in β are negligible, it is necessary to increase the values of K_{cyt} and $[B_{cyt}]$ appreciably. This is shown in the bottom plate of Fig. 6 for K_{cyt} = 150 μM and $[B_{cyt}] = 1.5 \cdot 10^4$ μM, where the value of β is now constant at $1/(1 + [B_{cyt}]/K_{cyt}) = 1/101$ as predicted by Eq. 24. With these parameters, the oscillations become identical to those in which buffering is treated with a constant parameter, β, having both an identical amplitude and sensitivity to $[IP_3]$ (De Young and Keizer, 1992; Li and Rinzel, 1994).

Estimates of K_{cyt} vary from less than 1 μM to more than 10 μM (Allbritton et al., 1992), whereas endogenous buffer site concentrations have been estimated in the range of 100–300 μM. Thus, the calculations with realistic values of K_{cyt} and $[B_{cyt}]$ (*top plate* of Fig. 6) suggest that buffering plays a significant role in cellular calcium oscillations. Indeed, because the factor β depends explicitly on $[Ca^{2+}]$, buffering does more than just rescale the time in Eq. 37 and could serve a function in controlling both cellular calcium oscillations and waves.

In these calculations, we have assumed that the Ca^{2+} buffers in the ER are of high capacity and low affinity, with $[B_{ER}]$ = 120,000 μM and K_{ER} = 1200 μM. These values are supported by recent experimental work (Milner et al., 1992). By varying these quantities (not shown), we have found that they, too, can modify the amplitude, frequency and existence of Ca^{2+} oscillations in this model. Thus, Ca^{2+} buffering on either side of the ER membrane would seem to be of potential importance for IP_3-induced signal transduction.

CONCLUDING REMARKS

By eliminating the concentrations of rapid buffers from the equations that describe the transport of Ca^{2+}, it is possible to define more clearly the effect of buffers on Ca^{2+} movements in cells. Although we have focused exclusively on buffers with independent, equivalent sites, the same type of analysis could be applied easily to other types of buffers. By combining our transport equation with the differential equations for slow buffers, our formalism also can be used to describe the combined action of fast and slow buffers. The explicit formulae that we obtain for the effective diffusion constant of Ca^{2+} under different conditions appear to be useful in analyzing experimental data in cell free extracts (Allbritton et al., 1992). Using these expressions in the presence of varying amounts of exogenous buffers, it might also be possible to extrapolate to the intrinsic diffusion constant of Ca^{2+} in situ.

The formalism is also useful in assessing the relative contributions of mobile and stationary buffers. However, because mobile buffers contribute a nondiffusive term to the Ca^{2+} transport equation (cf. Eq. 10), it is not always possible to define an effective diffusion constant for Ca^{2+} in the presence of mobile buffers (Zhou and Neher, 1993). For exogenous buffers such as fura-2, this effect becomes important at concentrations of the indicator above 1 μM, and at concentrations higher than 10 μM, the influence of fura-2 on diffusion is difficult to interpret. This argues in favor of using protocols with less mobile forms of indicators, such as fura-2 dextran, which should act more like stationary buffers.

Our primary interest in buffering is the influence of exogenous and endogenous buffers on Ca^{2+} oscillations and waves. Measurements in the cytoplasm suggest that in many cells about 99 out of every 100 Ca^{2+} ions in the cytoplasm are bound (Neher and Augustine, 1992; Tse et al., 1994). According to Eqs. 14, 15, and 37, this implies that both the effective diffusion constant of Ca^{2+} and its rate of influx or efflux into other compartments are reduced by a factor of about 0.01. This has a number of implications, not the least of which is that small percentage changes in the fraction of bound Ca^{2+} can strongly influence the rate of accumulation or depletion of free Ca^{2+}. Thus, a change of the fraction of bound Ca^{2+} from 0.99 to 0.98 actually doubles these rates. It is possible that cells use this feature to regulate the dynamics of Ca^{2+} movements.

Because the factor $\beta(c)$, which determines the effect of Ca^{2+} on the rates of Ca^{2+} influx and efflux, is actually dependent on $[Ca^{2+}]$, it has potential influence on Ca^{2+} oscillations and waves. Using our previous model of IP_3-induced Ca^{2+} oscillations (De Young and Keizer, 1992; Li and Rinzel, 1994), we have shown that changes in $\beta(c)$ can

modify, or even eliminate, Ca^{2+} oscillations when buffer characteristics are in the phenomenological range. These calculations make it clear that exogenous buffers can have similar effects, which provides a further caveat in the use of indicators to detect oscillations and might suggest additional applications of exogenous buffers as tools for exploring oscillations. Because Ca^{2+} buffers influence both fluxes and diffusion of free Ca^{2+} ions, they have an even greater potential significance for Ca^{2+} waves. This, and related results, will be reported in detail in a forthcoming publication.

APPENDIX A

Derivation of Eq. 10

We first obtain the differential equation for $[Ca^{2+}]_T$ by differentiating Eq. 9 with respect to time. Recalling that both $[Ca^{2+}]$ and $[B_m]_T$ depend on time, this gives

$$\frac{\partial[Ca^{2+}]_T}{\partial t} = \frac{1}{\beta}\frac{\partial[Ca^{2+}]}{\partial t} + \frac{[Ca^{2+}]}{[Ca^{2+}]+K_m}\frac{\partial[B_m]_T}{\partial t}. \tag{38}$$

Using Eq. 7 in place of the left hand side of Eq. 38, making use of Eq. 8 for $i = m$, and rearranging then gives an equation for $[Ca^{2+}]$ with the singular perturbations eliminated:

$$\frac{\partial[Ca^{2+}]}{\partial t} = \beta\left(D_{Ca}\nabla^2[Ca^{2+}] + D_{CaB_m}\nabla^2\frac{[B_m]_T[Ca^{2+}]}{[Ca^{2+}]+K_m}\right) - \frac{\beta[Ca^{2+}]}{[Ca^{2+}]+K_m}\frac{\partial[B_m]_T}{\partial t}. \tag{39}$$

This equation involves two variables, $[Ca^{2+}]$ and $[B_m]_T$. Adding together Eqs. 3 and 4, we can obtain the equation satisfied by $[B_m]_T$:

$$\frac{\partial[B_m]_T}{\partial t} = D_{B_m}\nabla^2[B_m]_T + \epsilon\nabla^2\frac{[B_m]_T[Ca^{2+}]}{[Ca^{2+}]+K_m}, \tag{40}$$

where $\epsilon = D_{CaB_m} - D_{B_m}$. Substituting this equation into the previous one then gives

$$\frac{\partial[Ca^{2+}]}{\partial t} = \beta\left(D_{Ca}\nabla^2[Ca^{2+}] + D_{CaB_m}\nabla^2\frac{[B_m]_T[Ca^{2+}]}{[Ca^{2+}]+K_m}\right) - \frac{\beta[Ca^{2+}]}{[Ca^{2+}]+K_m}\left(D_{B_m}\nabla^2[B_m]_T + \epsilon\nabla^2\frac{[B_m]_T[Ca^{2+}]}{[Ca^{2+}]+K_m}\right). \tag{41}$$

Eqs. 40 and 41 are the most general reduced equations for Ca^{2+} buffering.

These equations simplify if $\epsilon = 0$ and $[B_m]_T$ is initially uniform in space. Under these conditions, the second term in Eq. 40 vanishes and $[B_m]_T$ is, therefore, constant in time and space. This implies that the last term in Eq. 39 is zero and that the factor $[B_m]_T$ in the second term is a constant. Thus, the Laplacian becomes

$$\nabla^2\frac{[B_m]_T[Ca^{2+}]}{[Ca^{2+}]+K_m} = \gamma\left(\nabla^2[Ca^{2+}] - \frac{2}{K_m+[Ca^{2+}]}\nabla[Ca^{2+}]\cdot\nabla[Ca^{2+}]\right), \tag{42}$$

where

$$\gamma = \frac{K_m[B_m]_T}{(K_m+[Ca^{2+}])^2}. \tag{43}$$

Substituting this into the simplified Eq. 39 yields Eq. 10.

APPENDIX B

Generalization of Eq. 10 for multiple buffers

Under the assumption of rapid equilibrium for all of the buffers, the algebraic manipulations leading to Eq. 10 remain valid for each of the buffer species. As a consequence, it is easy to show that the equation satisfied by the free Ca^{2+} concentration is

$$\frac{\partial[Ca^{2+}]}{\partial t} = \bar{\beta}\left(D_{Ca} + \sum_j \gamma_j D_{m_j}\right)\nabla^2[Ca^{2+}] - 2\bar{\beta}\sum_j \frac{\gamma_j D_{m_j}}{K_{m_j}+[Ca^{2+}]}\nabla[Ca^{2+}]\cdot\nabla[Ca^{2+}], \tag{44}$$

where the generalization of the factor β is

$$\bar{\beta} = \left(1 + \sum_i \frac{K_{s_i}[B_{s_i}]_T}{(K_{s_i}+[Ca^{2+}])^2} + \sum_j \frac{K_{m_j}[B_{m_j}]_T}{(K_{m_j}+[Ca^{2+}])^2}\right)^{-1} \tag{45}$$

and the generalizations of the factor γ are

$$\gamma_j = \frac{K_{m_j}[B_{m_j}]_T}{(K_{m_j}+[Ca^{2+}])^2}. \tag{46}$$

These equations generalize Eq. 10 and can be used in the same fashion.

APPENDIX C

Buffering in the De Young-Keizer model

Using Eq. 37, it is possible to introduce the effect of Ca^{2+} buffers into Li's simplication of the De Young-Keizer model (Li and Rinzel, 1994). This leads to the following equations:

$$\frac{dw}{dt} = \frac{w_\infty - w}{\tau_{Ca}} \tag{47}$$

$$\frac{d[Ca^{2+}]}{dt} = \frac{\beta}{\tau}\left\{ c_1\left[v_1\left(\frac{w[Ca^{2+}]}{d_5+[Ca^{2+}]}\right)^3 + v_2\right]([Ca^{2+}_{ER}] - [Ca^{2+}]) \tag{48}$$

$$- v_3\left(\frac{[Ca^{2+}]^2}{k_3^2+[Ca^{2+}]^2}\right)\Big\}, \tag{49}$$

where the indicated functions are

$$\alpha = \frac{[IP_3]+d_1}{[IP_3]+d_3}, \tag{50}$$

$$w_\infty = \left(\frac{[IP_3]}{[IP_3]+d_3}\right)\left(\frac{d_2}{\alpha d_2+[Ca^{2+}]}\right), \tag{51}$$

$$\tau_{Ca} = \frac{1}{a_2(\alpha d_2+[Ca^{2+}])}, \tag{52}$$

$$f_{cyt} = \left(1 + \frac{[B_{cyt}]}{K_{cyt}+[Ca^{2+}]}\right)^{-1}, \tag{53}$$

$$\beta = \left(1 + \frac{K_{cyt}[B_{cyt}]}{(K_{cyt}+[Ca^{2+}])^2}\right)^{-1}, \tag{54}$$

$$b = K_{ER} + [B_{ER}] - \frac{c_0 - [Ca^{2+}]/f_{cyt}}{c_1}, \tag{55}$$

$$[Ca^{2+}_{ER}] = \tfrac{1}{2}(-b + \sqrt{b^2 + 4K_{ER}(c_0 - [Ca^{2+}]/f_{cyt})/c_1}). \tag{56}$$

Here we have used K_{cyt} and $[B_{cyt}]$ for the dissociation constant and buffer site concentration in the cytosol, and K_{ER} and $[B_{ER}]$ for the dissociation constant and buffer site concentration in the ER. Explicit inclusion of buffering effects modifies the expression (De Young and Keizer, 1992) for $[Ca^{2+}_{ER}]$, whose dependence on $[Ca^{2+}]$ now comes from solving the quadratic equation for conservation of total Ca^{2+}, and introduces the factor, β, into Eq. 49. The scale factor τ in Eq. 49 compensates for the fact that the buffering term, β, was absorbed into the constants v_1, v_2, and v_3 in earlier work (De Young and Keizer, 1992; Li and Rinzel, 1994). Choosing $\tau = 0.01$ permits us to retain the previous values (De Young and Keizer, 1992) of all the parameters in the model: $d_1 = 0.13\ \mu M\ s^{-1}$; $d_2 = 1.05\ \mu M\ s^{-1}$; $d_3 = 0.943\ \mu M\ s^{-1}$; $d_5 = 0.0823\ \mu M\ s^{-1}$; $a_2 = 0.2\ s^{-1}$; $c_0 = 2.0\ \mu M$; $c_1 = 0.185$; $v_1 = 6\ s^{-1}$; $v_2 = 0.11\ s^{-1}$; $v_3 = 0.9\ \mu M\ s^{-1}$; $k_3 = 0.1\ \mu M$. The remaining parameter values are given in Fig. 6.

This work was supported by National Science Foundation grants BIR 9214381, BIR 9300799, and the Agricultural Experiment Station of the University of California, Davis. We thank Saleet Jafri, Greg Smith, and Paul Smolen for helpful discussion.

REFERENCES

Allbritton, N. L., T. Meyer, and L. Stryer. 1992. Range of messenger action of calcium ion and inositol 1,4,5-trisphosphate. *Science.* 258:1812–1815.

Berridge, M. J. 1989. *In* Cell to Cell Signalling from Experiments to Theoretical Models. A. Goldbeter, editor. Academic Press, New York. 449–459.

Bezprozvanny, I., J. Watras, and B. E. Ehrlich. 1991. Bell-shaped calcium response curves of Ins(1,4,5)P_3- and calcium-gated channels from endoplasmic reticulum of cerebellum. *Nature.* 351:751–754.

Blumenfeld, H., L. Zablow, and B. Sabatini. 1992. Evaluation of cellular mechanisms for modulation of calcium transients using a mathematical model of fura-2 Ca^{2+} imaging in aplysia sensory neurons. *Biophys. J.* 63:1146–1164.

Chad, J. E., and R. Eckert. 1984. Calcium domains associated with individual channels can account for anomalous voltage relations of Ca-dependent responses. *Biophys. J.* 45:993–999.

De Young, G., and J. Keizer. 1992. A single-pool inositol 1,4,5-trisphosphate-receptor-based model for agonist-stimulated oscillations in Ca concentration. *Proc. Natl. Acad. Sci.* USA. 89:9895–9899.

Eckert, R., and J. E. Chad. 1984. Inactivation of calcium channels. *Biophys. Mol. Biol.* 44:215–267.

Finch, E. A., T. J. Turner, and S. M. Goldin. 1991. Calcium as a coagonist of inositol 1,4,5-trisphosphate induced calcium release. *Science.* 252:443–446.

Fogelson, A., and R. Zucker. 1985. Presynaptic calcium diffusion from various arrays of single channels. *Biophys. J.* 48:1003–1017.

Hernandez-Cruz, A., F. Sala, and P. R. Adams. 1990. Subcellular calcium transients visualized by confocal microscopy in a voltage-clamped vertebrate neuron. *Science* 247:858–862.

Hodgkin, A. L., and R. D. Keynes. 1957. Movements of labelled calcium in squid giant axons. *J. Physiol.* 138:253–281.

Kao, J. P. Y., and R. Y. Tsien. 1988. Ca binding kinetics of fura-2 and azo-1 from temperature-jump relaxation measurements. *Biophys. J.* 53:635–639.

Keizer, J. 1987. Statistical Thermodynamics of Nonequilibrium Processes. Springer-Verlag, New York. 506 pp.

Keizer, J., and G. De Young. 1994. Simplification of a realistic model of IP_3-induced Ca oscillations. *J. Theor. Biol.* 166:431–442.

Lechleiter, J. D., and D. E. Clapham. 1992. Molecular mechanisms of intracellular calcium excitability in *X. laevis* oocytes. *Cell.* 69:283–294.

Li, Y.-X., and J. Rinzel. 1994. Equations for $InsP_3$ receptor-mediated $[Ca^{2+}]_i$ oscillations derived from a detailed kinetic model: a Hodgkin-Huxley like formalism. *J. Theor. Biol.* 166:461–473.

Li, Y.-X., J. Rinzel, J. Keizer, and S. S. Stojilkovic. 1994. Calcium oscillations in pituitary gonadotrophs: comparison of experiment and theory. *Proc. Natl. Acad. Sci.* USA. 91:58–62.

Llinas, R., M. Sugimori, and R. B. Silver. 1992. Microdomains of high calcium concentration in a presynaptic terminal. *Science.* 256:677–679.

Meyer, T., and L. Stryer. 1991. Calcium spiking. *Annu. Rev. Biophys. Biophys. Chem.* 20:153–174.

Milner, R. E., K. S. Famulski, and M. Michalak. 1992. Calcium binding proteins in the sacroplasmic/endoplasmic reticulum of muscle and non-muscle cells. *Mol. Cell. Biochem.* 112:1–13.

Mironov, S. L. 1990. Theoretical analysis of Ca wave propagation along the surface of intracellular stores. *J. Theor. Biol.* 146:87–97.

Miyazaki, S., M. Yuzaki, K. Nakada, H. Shirakawa, S. Nakanishi, S. Nakade, and K. Mikoshiba. 1992. Block of Ca^{2+} wave and Ca^{2+} oscillation by antibody to the inositol 1,4,5-trisphosphate receptor in fertilized hamster eggs. *Science.* 257:251–255.

Murray, J. D. 1989. Mathematical Biology. Springer-Verlag, New York. 767 pp.

Neher, E., and G. J. Augustine. 1992. Calcium gradients and buffers in bovine chromaffin cells. *J. Physiol.* 450:273–301.

Nowycky, M. C., and M. J. Pinter. 1993. Time courses of calcium and calcium-bound buffers following calcium influx in a model cell. *Biophys. J.* 64:77–91.

Nuccitelli, R., D. L. Yim, and T. Smart. 1993. The sperm-induced Ca^{2+} wave following fertilization of the *Xenopus* egg requires the production of ins-(1,4,5)p(3). *Dev. Biol.* 158:200–212.

Roberts, W. M. 1993. Spatial calcium buffering in saccular hair cells. *Nature.* 363:74–76.

Roberts, W. M. 1994. Localization of calcium signals by a mobile calcium buffer in frog saccular hair cells. *J. Neurosci.* 14:3246–3262.

Sala, F., and A. Hernandez-Cruz. 1990. Calcium diffusion in a spherical neuron. *Biophys. J.* 57:313–324.

Sherman, A., J. Keizer, and J. Rinzel. 1990. Domain model for Ca^{2+}-inactivation of Ca^{2+} channels at low channel density. *Biophys. J.* 58: 985–995.

Simon, S. M., and R. R. Llinas. 1985. Compartmentalization of the submembrane calcium activity during calcium influx and its significance in transmitter release. *Biophys. J.* 48:485–498.

Stern, M. D. 1992. Buffering of calcium in the vicinity of a channel pore. *Cell Calcium.* 13:183–192.

Stojilkovic, S. S., M. Kukuljan, M. Tomic, E. Rojas, and K. J. Catt. 1993. Mechanism of agonist-induced $[Ca^{2+}]_i$ oscillations in pituitary gonadotrophs. *J. Biol. Chem.* 268:7713–7720.

Timmerman, M. P., and C. C. Ashley. 1986. Fura-2 diffusion and its use as an indicator of transient free calcium changes in single striated muscle cells. *FEBS Lett.* 209:1–8.

Tse, A., and B. Hille. 1991. Gnrh-induced Ca^{2+} oscillations and rhythmic hyperpolarization of pituitary gonadotrophs. *Science.* 255:462–464.

Tse, A., F. W. Tse, and B. Hille. 1994. Calcium homeostasis in identified rat gonadotropes. *J. Physiol.* In Press.

Zhou, Z., and E. Neher. 1993. Mobile and immobile calcium buffers in bovine adrenal chromaffin cells. *J. Physiol.* 469:245–273.